

Attenuation of Fundamental Longitudinal Guided Wave Mode in Steel Pipes Embedded in Soil

Juwon Lee*, Sung Woo Shin**† and Won-Bae Na*

Abstract In this study, characteristics of the fundamental longitudinal guided wave mode, $L(0,1)$, which is a usual mode employed in the inspection of the above-ground pipe, of the buried pipe were numerically investigated considering property changes in the surrounding soil. Results showed that soil conditions are significantly affecting the attenuation of $L(0,1)$ mode in the pipe embedded in soil. Especially, if the soil is partially saturated, the attenuation of $L(0,1)$ mode is larger and is very similar regardless of the degree of water saturation in the surrounding soil. However, when the soil is fully saturated, the attenuation of $L(0,1)$ mode is less and show different trend with its partially saturated counterparts.

Keywords: Guided Waves, NDT of Buried Pipes, Mode Attenuation, Waves in Soil

1. Introduction

Pipes are industrial structures used for long range transportation of fluidic products such as gas and water. Like other industrial structures, these pipes are damaged by unexpected events and deteriorated with time. Therefore, a periodic inspection or monitoring of the pipe is important for the assessment of their safety and service-ability. Unfortunately, however, if the pipes are buried in underground, the inspection task is often cumbersome or sometimes impossible due to the presence of a surrounding soil.

Many nondestructive testing techniques have been proposed and developed for the inspection of the pipelines. Among them, guided wave based technique has been emerged as a promising tool for the inspection of the pipes (Rose, 2002). When the pipe is exposed to the air such as an above-ground pipe, the guided

wave generated in this pipe can propagate very long range without much loss of its energy. Owing to this property, the guided wave based technique has been successfully implemented for the inspection of the above-ground pipelines. However, it is challenging to apply this technique for the effective inspection of the buried underground pipes due to rapid attenuation of wave energy in the buried pipes. Energy losses of the guided waves in the buried pipe can cause from material damping of the pipe itself and wave transmission (leakage) loss to the surrounding soil (Rose, 2004). Especially, transmission loss of the energy is depending on wave mode and frequency and on the properties of the surrounding soil such as bulk wave velocities so that the behavior of the guided wave in the buried pipe can be very complex.

In this study, characteristics of the fundamental longitudinal guided wave mode,

L(0,1), which is usual mode employed in the inspection of the above-ground pipe, of the buried gas-filled pipe are numerically investigated considering soil property changes in the surrounding soil. To this end, the steel pipe embedded in a soil is numerically modeled using the global matrix method. Constitutive relation considering the degree of water saturation of the surrounding soil is derived and applied to the numerical model to see the effect of soil conditions on the wave behavior. Numerical analysis is performed to find solutions of the global matrix model of the buried pipe and results are discussed.

2. Technical Basis

2.1 Attenuation Calculation of Guided Wave in Buried Pipe

Guided wave modal solutions, which contain propagation properties such as phase velocity, can be analytically obtained for a pipe in traction-free condition using Gazis' solution(Gazis, 1958). However, since closed-form modal solutions for the pipe embedded in a soil are not available, the solutions must be sought in a numerical model. For this, the global matrix method(Lowe, 1995) is employed to model the pipe embedded in soil.

For the construction of the global matrix model of a pipe embedded in soil, it is considered as an axi-symmetric multi-layered system as shown in Fig. 1. A steel pipe (wall thickness: 6 mm, inner radius: 51 mm), normally used in petrochemical industry, is selected(ANSI/API Spec 5L, 2007). Each outer wall of the pipe is surrounded by infinite soil half space. Infinite soil space is assumed since the depth of the buried pipe from the ground level is normally more than 1.5 m (Monahan, 1994) and wave attenuation in a soil is very rapid so that no reflection is expected from the soil-air interface. At the pipe-soil interface, it is

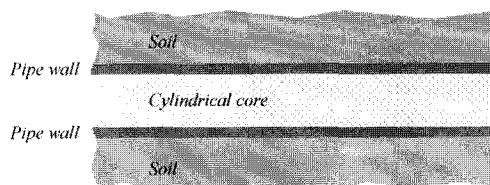


Fig. 1 Multi-layered model for buried steel pipe

assumed to have no relative motion, since, in ultrasonic testing, the wave amplitude in the outer pipe wall is very small so that the force acting on the interface is sufficiently less than static friction resistance of the interface. For a layer inside the pipe (transporting fluid layer), gas-filled condition is considered in this study. Moreover, since the acoustical impedance of gaseous material is very low comparing with steel pipe, it may be sufficient to assume the gas-filled condition as a vacuum state. Using the global matrix method(Lowe, 1995), a wave propagation model of the buried pipe with no external forces can be formulated as:

$$[M]\{A\} = \{0\} \quad (1)$$

where $[M]$ is the global matrix of the buried pipe and $\{A\}$ is a vector of the partial wave amplitudes(Lowe, 1995). The global matrix $[M]$ is assembled from all layer interface matrices, which are expressed as a function of the material properties, the frequency, and the wave number, describing the displacement and stress fields associated with harmonic wave propagation along the multi-layered system. Eqn. (1) is satisfied if the determinant of the global matrix is zero as

$$f(\omega, k) = \det[M] = 0 \quad (2)$$

Eqn. (2) is known as characteristic equation or dispersion equation(Lowe, 1995). The solutions of eqn. (2) are found by numerical searches for the frequency (ω) and complex wave number (k) pairs. Thus the numerical solution of the

buried pipe (i.e. multi-layered system) is in three variables: real frequency (ω), real wave number (k_{re}) and imaginary wave number (k_{im}). The attenuation due to leakage of guided wave mode can then be calculated from the ratio between the imaginary part and the real part of the complex wave number solution as

$$\kappa = 2\pi \frac{k_{im}}{k_{re}} \quad (3)$$

where κ is in nepers per wavelength, so that a wave of unit amplitude is reduced to an amplitude of $e^{-\kappa}$ after travelling one wavelength (Lowe, 1995). In this study, a commercial solver, DISPERSE[®], is used to find solutions in the complex wave number domain and to calculate the attenuation curve (Pavlakovic and Lowe, 2003).

2.2 Soil Constitutive Model

Guided waves propagating in the pipe embedded in soil attenuate due to the presence of the surrounding soil. A surrounding medium in a multi-layered system absorbs wave energy. The amount of the energy absorption varies with the material properties (density and P- and S-wave velocities) of a surrounding medium (Rose, 2004). Unfortunately, the determination of the material properties of a soil is not an easy task. Since a soil is generally granular and porous medium, the properties of the soil greatly depend on many factors such as the state of the water saturation, porosity, to name a few (Hardin and Blandford, 1989). Especially, since the mechanical behavior of the soil is extremely different when it saturated with water or not, the degree of water saturation has been identified one of the most important factors that governs the properties of the soil (Santamarina, 2001). Therefore, in order to determine the soil properties considering the degree of water saturation, a constitutive relationship is derived in this study using elastic wave propagation

theory. Note that, in order to consider merely the effect of the water saturation on the soil properties, the porosity remains constant in this derivation procedure while the water content increases in the soil.

Using an effective solid continuum concept, the compression wave velocity ($C_{P,soil}$), and the shear wave velocity ($C_{S,soil}$) of the soil can be expressed in the form as follows (Santamarina, 2001):

$$C_{P,soil} = \sqrt{\frac{B_{soil} + \frac{4}{3}G_{soil}}{\rho_{soil}}} \quad (4)$$

$$C_{S,soil} = \sqrt{\frac{G_{soil}}{\rho_{soil}}} \quad (5)$$

where B_{soil} and G_{soil} denote the effective bulk and shear moduli respectively and ρ_{soil} the bulk density of soil. The bulk density (ρ_{soil}) is defined as

$$\rho_{soil} = \rho_s(1-n) + \rho_w \cdot n \cdot S + \underbrace{\rho_a \cdot n \cdot (1-S)}_{\approx 0} \quad (6)$$

where ρ_s is density of soil mineral, ρ_w and ρ_a are the densities of the water and the air respectively, n is the porosity, and S is the degree of water saturation.

If a soil consists of a granular skeleton and pore fluids (usually water and air), then the shear and bulk modulus, G_{soil} and B_{soil} , of a soil involves the contribution of the different soil components: the stiffness of soil mineral, the stiffness of the fluid, the stiffness of the soil-fluid suspension, and the stiffness of the skeleton (Santamarina, 2001). However, the shear modulus, G_{soil} , of a soil remains unaffected by the presence of the fluid. Therefore, at the same effective stress,

$$G_{soil} \cong G_{sk} \quad (7)$$

where G_{sk} is the shear modulus of the soil skeleton (FratTA et al., 2005). On the other hand,

since the bulk modulus is largely affected by the presence of the fluid, it can be decomposed as (Santamarina, 2001):

$$B_{soil} = B_{sk} + B_{sus} \quad (8)$$

where B_{sk} is the bulk modulus of the soil skeleton and B_{sus} is the bulk modulus of soil-fluid suspension defined as (Santamarina, 2001):

$$B_{sus} = \left(\frac{n}{B_{fl}} + \frac{1-n}{B_g} \right)^{-1} \quad (9)$$

where B_g is the bulk modulus of the soil mineral grains and B_{fl} is the bulk modulus of the pore fluid defined as (Santamarina, 2001) :

$$B_{fl} = \left(\frac{S}{B_w} + \frac{1-S}{B_a} \right)^{-1} \quad (10)$$

where B_w is the bulk modulus of the water ($\approx 2.2GPa$) and B_a is the bulk modulus of the air ($\approx 142kPa$) (Santamarina, 2001). Therefore, eqn. (8) can be rewritten using eqns. (9) and (10) as:

$$B_{soil} = B_{sk} + \left(n \left(\frac{S}{B_w} + \frac{1-S}{B_a} \right) + \frac{1-n}{B_g} \right)^{-1} \quad (11)$$

In eqn. (9), the remaining term to be defined is the bulk modulus of soil skeleton (B_{sk}). Fratta et al. (Fratta et al., 2005) proposed and validated a following relationship for the bulk skeleton modulus of a soil.

$$B_{sk} = G_{soil} \frac{2}{3} \frac{1+\nu}{1-2\nu} \quad (12)$$

where ν is the Poisson's ratio (normally 0.10-0.15 for elastic wave propagation in soil). Therefore, if an effective stress of a soil remains constant, eqn. (12) can be rewritten using eqn. (7) as

$$B_{sk} \cong G_{sk} \frac{2}{3} \frac{1+\nu}{1-2\nu} \quad (13)$$

Finally, if the porosity and the effective stress of a soil remain constant, then the bulk density ρ_{soil} (eqn. 6), the compression wave velocity $C_{P,soil}$ (eqn. 4), the shear wave velocity $C_{S,soil}$ (eqn. 5) can be expressed as functions of the degree of water saturation as:

$$\rho_{soil}(S) = \rho_s(1-n) + \rho_w \cdot n \cdot S \quad (14)$$

$$C_{P,soil}(S) = \sqrt{\frac{n \left(\frac{S}{B_w} + \frac{1-S}{B_a} \right) + \frac{1-n}{B_g} + G_{sk} \left(\frac{2(1-\nu)}{1-2\nu} \right)}{\rho_s(1-n) + \rho_w \cdot n \cdot S}} \quad (15)$$

$$C_{S,soil}(S) = \sqrt{\frac{G_{sk}}{\rho_s(1-n) + \rho_w \cdot n \cdot S}} \quad (16)$$

It should be noted that, as seen in eqns. (15) and (16), the shear modulus of soil skeleton G_{sk} is very important in determination of two velocities. G_{sk} depends on the type of soil, porosity, stress history, matric suction, the amplitude of the applied load, confinement pressure, etc. and normally varies from 10-50(MPa) (Fratta et al. 2005; Qian et al, 1993). The effectiveness of the eqns. (14-16) are discussed in a subsequent chapter.

3. Selection of Material Properties for Mode Attenuation Analysis of Buried Pipe

Material properties for the steel pipe are shown in Table 1. For the surrounding soil, a well-graded sandy soil, which is recommended as a back-fill material in an underground pipe construction guideline (Monahan, 1994), is chosen. The constants, will be used to calculate the properties (ρ_{soil} , $C_{P,soil}$, and $C_{S,soil}$) of the sandy soil, are shown in Tables 2, 3 and 4. Note that the constants are obtained from the previous research (Fratta et al. 2005; Qian et al, 1993).

The properties (ρ_{soil} , $C_{P,soil}$, and $C_{S,soil}$) of the sandy soil as a function of the degree of water saturation were calculated using the eqns. 14-16 and the constants, and the results are

Table 1 Steel properties

Density (kg/m^3)	P-wave velocity (m/s)	S-wave velocity (m/s)
7100	4500	2500

Table 2 Bulk modulus for each component in sandy soil (MPa)

Air (B_a)	Water (B_w)	Sand Mineral (B_g)	Shear Modulus of Soil Skeleton (G_{sk})
0.142	2190	3500	25

Table 3 Densities of sand mineral and water (kg/m^3)

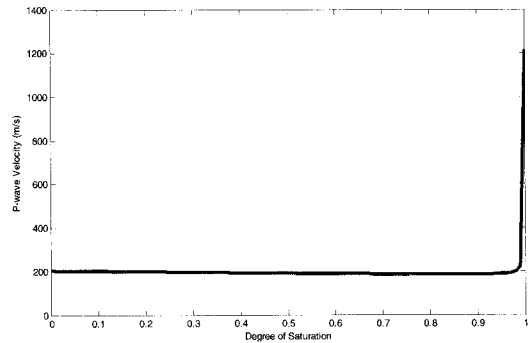
Sand Mineral (ρ_s)	Water (ρ_w)
2650	1000

Table 4 Dimensionless soil parameters

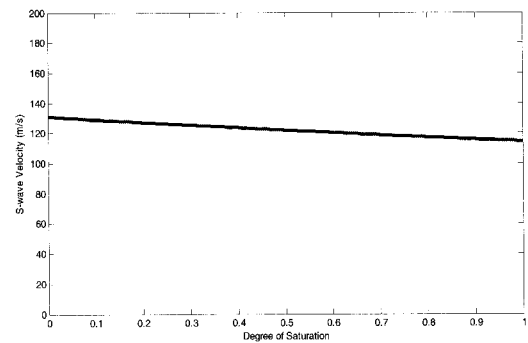
Porosity (n)	Poisson's Ratio of Soil (ν)
0.45	0.15

shown in Fig. 2. It is seen that P-wave velocity suddenly increases when the degree of saturation is close to 1.0. For wet sand, any presence of air will reduce the velocity considerably since the compressibility of the soil is dominated by the air. This extreme behavior of the P-wave velocity of the sandy soil can also be found in previous study. For example, the predicted and estimated P-wave velocity of medium grain size sand is about 1600 m/s when it is fully saturated, and about 16 m/s when it is fully dried (Bachrach and Nur, 1998). On the other hand, the S-wave velocity decreases very slightly as the saturation increases. This moderate behavior of S-wave is mainly due that the shear stiffness of a soil remains unaffected by the presence of the fluid. Similar results for S-wave velocity behavior can be found in the previous study (Fratta et al., 2005). Finally, the mass density of sandy soil gradually increases as the saturation increases. Reported results on the wave velocity of the sandy soil (Fratta et al.

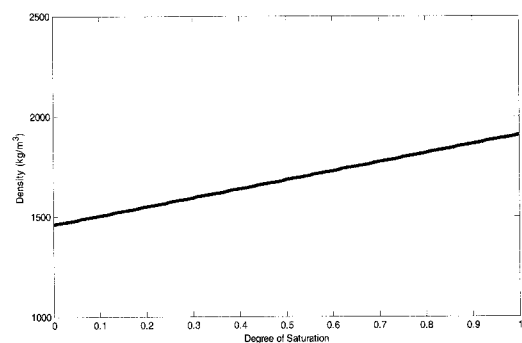
2005; Bachrach and Nur, 1998). validate the effectiveness of the proposed constitutive equations to predict typical material properties of a soil with respect to the degree of water saturation. In this study, material properties of the sandy soil for mode attenuation analysis of buried steel pipe were selected at 10 %, 50 %, 90 %, and 100 % of the degrees of saturation and listed in Table 5.



(a)



(b)



(c)

Fig. 2 Soil property variations with respect to degree of water saturation; (a) P-wave velocity, (b) S-wave velocity, (c) Density

Table 5 Material properties of soil with saturation degrees

Degree of Saturation	Density (kg/m ³)	P-wave velocity (m/s)	S-wave velocity (m/s)
0.1	1498	202	129
0.5	1678	191	122
0.9	1862	185	116
1.0	1903	1216	114

4. Mode Attenuation Analysis

The solutions (frequency and complex wave number) for L(0,1) mode of the buried pipe embedded in soil were numerically found using DISPERSE software. The solutions found are then used to calculate the attenuation of the L(0,1) mode by eqn. (3). It is worth noting that only L(0,1) mode is chosen for analysis because it is known one of the most important modes in guided wave based pipe inspection. Since this study is concerned solely with the behavior of L(0,1) mode in the buried pipe, other fundamental modes such as flexural, F(1,1), and torsional, T(0,1), are not considered here and remained for future study.

Fig. 3 shows the attenuation of L(0,1) mode in the buried pipe for various degrees of water saturation in the surrounding soil. It is seen that 10 %, 50 %, and 90 % saturation cases show very similar attenuation trend while 100 % case show solely different behavior. However, for all cases, a sudden increase of attenuation is seen at low frequency region (<30 kHz) and mild attenuation behaviors are seen a frequency range larger than 30 kHz. At very low frequency region (<10 kHz), attenuation is very low (almost zero) for all cases, and which is due that wave motion of L(0,1) mode in this region is in the axial and not the radial direction. Therefore, wave energy does not leak much into surrounding medium in this region. It is also observed that the level of attenuation for 100 % case is generally lower than other degrees of saturation cases. This suggests that L(0,1) mode

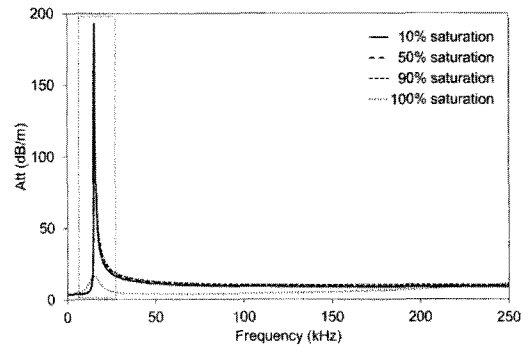


Fig. 3 Attenuations of L(0,1) mode in the buried pipe for various degrees of saturation in surrounding soil

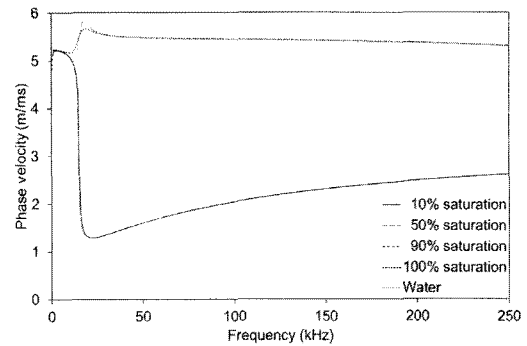


Fig. 4 Phase velocity dispersion of L(0,1) mode in the buried pipe for various conditions on surrounding medium

in the pipe embedded in fully saturated soil will propagate longer distance than in partially saturated soil. In order to investigate this unique behavior of 100 % case, phase velocity dispersion curves for all cases are plotted in Fig. 4. Note that the pipe surrounded by water case (P-wave velocity : 1450 m/s) is also provided for comparison with soil surrounding cases.

It is observed that phase velocity behaviors of L(0,1) mode of the pipe both embedded in 100 % saturated soil and in water show very similar trend. This means that when the surrounding soil is fully saturated with water, it behaves like water. This also suggest that P-wave velocity of the surrounding medium greatly affects L(0,1) mode behavior in the embedded pipe. As shown in Fig. 2, P-wave

velocity of 100 % saturated soil (1216 m/s) is very close to P-wave velocity of water (1450 m/s). However, since the compressibility of the soil is dominated by the air, P-wave velocities of partially saturated soils (10%, 50%, 90%) are very low (about 200 m/s) due to presence of the air in void and those are not much change with the saturation degrees. This confirms why L(0,1) mode behaviors in partially saturated soil cases are very similar. Moreover, it is also confirmed that (comparing with P-wave velocity of the soil) S-wave velocity and density of the surrounding soil are not major factors to govern L(0,1) mode behavior in the buried pipe.

Fig. 5 shows detailed attenuation behaviors in frequency range from 10 to 20 kHz. It is seen that attenuation levels for partially saturated soil cases reach very high (almost 180 dB/m) around 15 kHz, while no significant attenuation variation is seen for fully saturated soil case. Such transition is also observed in phase velocity dispersion in Fig. 4. This means radial wave motion, which is major motion to transmit wave energy into surrounding medium, of the pipe embedded in the partially saturated soils are very large comparing with that of in the fully saturated soil. Fig. 6 show relative displacement profiles of radial component at 15 kHz in the pipe wall for all saturation cases. It is seen that the magnitudes for partially saturated soil cases are larger than the fully saturated soil case and this result confirms the larger attenuation behavior (in the vicinity of 15 kHz) of L(0,1) mode in the partially saturated soil.

On the other hand, at a higher frequency region, attenuation is not as high as in the low frequency region as shown in Fig. 7, although the levels are still different with the degrees of water saturation in the surrounding soil. Interestingly, at this frequency region, the attenuation generally decreases as frequency increases for the partially saturated soil cases, but it increases as frequency increases for the fully saturated soil. However, an inverse relation

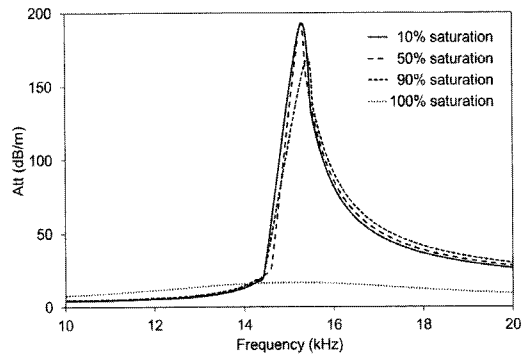


Fig. 5 Detailed attenuation behaviors of L(0,1) mode in the frequency range from 10 to 20 (kHz)

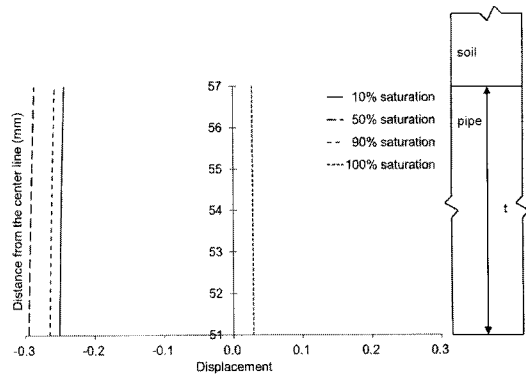


Fig. 6 Relative displacement profiles of radial component in the pipe wall at 15 kHz

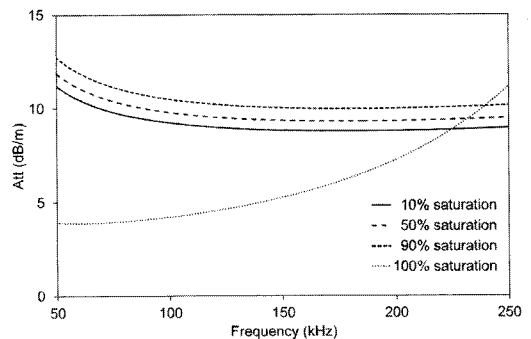


Fig. 7 Detailed attenuation behaviors of L(0,1) mode in the frequency range from 50 to 250 (kHz)

is observed for phase velocity dispersion. As shown in Fig. 4, at this frequency region, phase velocity increases as frequency increases for the partially saturated soil cases, while that for the fully saturated soil case decreases as frequency

increases. Especially the level of attenuation for fully saturated case exceeds those for the partially saturated cases at frequency 250 kHz. This result suggests that L(0,1) behavior in the pipe embedded in soil is very complex so that careful consideration on the conditions of the surrounding soil are needed in selection of excitation frequency of L(0,1) mode for the effective application of guided wave techniques for an inspection of buried pipes.

Conclusions

In this study, guided wave attenuation characteristics in the buried pipes were investigated for various water saturation conditions in surrounding soil. Soil constitutive relation was developed and guided wave mode attenuation analysis was performed. Results showed that soil conditions are significantly affecting the attenuation of L(0,1) mode in the pipe embedded in soil. Especially, if the soil is partially saturated, the behaviors are very similar each other regardless of the degree of water saturation in the surrounding soil. However, when the soil is fully saturated, the attenuation of L(0,1) mode shows totally different trend with its partially saturated counterparts. Moreover, L(0,1) mode behavior in the pipe surrounded by fully saturated soil is very similar with that of the pipe surrounded by water. It is also found that, comparing with P-wave velocity of the soil, S-wave velocity and density of the surrounding soil are not major factors to govern L(0,1) mode behaviors in the buried pipe.

Acknowledgement

This work was supported by the Innovation Center for Safety Diagnosis Technology of Heavy and Chemical Facilities of Chonnam National University through a Regional Innovation Center (RIC) program of the Korean Ministry of Knowledge and Economics (MKE).

References

- ANSI/API Spec 5L : Specification for Line Pipe, American Petroleum Institute, 2007
- Bachrach, R. and Nur, A. (1998) High-Resolution Shallow-Seismic Experiments in Sand, Part I : Water Table, Fluid Flow, and Saturation," *Geophysics*, Vol. 63(4), pp. 1225-1233
- Fratta, D., Alshibli, K. A., Tanner, W. M. and Roussel, L. (2005) Combined TDR and P-wave Velocity Measurements for the Determination of In Situ Soil Density – Experimental Study, *Geotechnical Testing Journal*, Vol. 28(6), pp. 1-11
- Gazis, D. C. (1958) Exact Analysis of the Plane-Strain Vibrations of Thick-walled Hollow Cylinders, *Journal of Acoustical Society of America*, Vol. 31, pp. 568-578
- Hardin, B. O. and Blandford, G. E. (1989) Elasticity of Particulate Materials, *ASCE Journal of Geotechnical Engineering*, Vol. 115(6), pp. 788-805
- Lowe, M. J. S. (1995) Matrix Technique for Modelling Ultrasonic Waves in Multilayered Media, *IEEE Transactions on Ultrasonics, Ferroelectrics and Frequency Control*, Vol. 42(4), pp. 525-542
- Monahan, E. J. (1994) *Construction of Fills : 2nd Edition*, John Wiley and Sons
- Pavlakovic, B. and Lowe, M. J. S. (2003) *DISPERSE USER MANUAL : A System for Generating Dispersion Curves*, Department of Mechanical Engineering, Imperial College, University of London
- Qian, X., Gray, D. H. and Woods, R. D. (1993) Voids and Granulometry: Effects on Shear

Modulus of Unsaturated Sands, *ASCE Journal of Geotechnical Engineering*, Vol. 119(2), pp. 295-314

Rose, J. L. (2002) A Baseline and Vision of Ultrasonic Guided Wave Inspection Potential, *Journal of Pressure Vessel Technology*, Vol. 124(3), pp. 273-283

Rose, J. L. (2004) *Ultrasonic Waves in Solid Media*, Cambridge University Press

Santamarina, J. C. (2001) *Soils and Waves*, John Wiley & Sons